

Detection of blueshifted emission and absorption and a relativistic Iron line in the X-ray spectrum of ESO 323-G077 ^{*}

E. Jiménez-Bailón^{1,2†}, Y. Krongold¹, S. Bianchi³, G. Matt³, M. Santos-Lleó⁴,
E. Piconcelli⁵, N. Schartel⁴

¹ *Instituto de Astronomía, Universidad Nacional Autónoma de México, Apartado Postal 70-264, 04510 Mexico DF, Mexico*

² *LAEFF-INTA, Apartado 50727, 28080 Madrid, Spain*

³ *Universita Roma Tre, Via della Vasca Navale 64, I-00146, Roma, Italy*

⁴ *XMM-Newton Science Operation Centre, ESAC, ESA, Apartado. 50727, 28080 Madrid, Spain*

⁵ *Osservatorio Astronomico di Roma (INAF), Via Frascati, 33, 00040, Monteporzio Catone, Italy*

Accepted 1988 December 15. Received 1988 December 14; in original form 1988 October 11

ABSTRACT

We report on the X-ray observation of the Seyfert 1 galaxy ESO 323-G077 performed with *XMM-Newton*. The *EPIC* spectra show a complex spectrum with conspicuous absorption and emission features. The continuum emission can be modelled with a power law with an index of 1.99 ± 0.02 in the whole *XMM-Newton* energy band, marginally consistent with typical values of Type-I objects. An absorption component with an uncommonly high equivalent Hydrogen column ($n_H = 5.82_{-0.11}^{+0.12} \times 10^{22} \text{ cm}^{-2}$) is affecting the soft part of the spectrum. Additionally, two warm absorption components are also present in the spectrum. The lower ionised one, mainly imprinting the soft band of the spectrum, has an ionisation parameter of $\log U = 2.14_{-0.07}^{+0.06}$ and an outflowing velocity of $v = 3200_{-200}^{+600} \text{ km/s}$. Two absorption lines located at ~ 6.7 and $\sim 7.0 \text{ keV}$ can be modelled with the highly ionised absorber. The ionisation parameter and outflowing velocity of the gas measured are $\log U = 3.26_{-0.15}^{+0.19}$ and $v = 1700_{-400}^{+600} \text{ km/s}$, respectively. Four emission lines were also detected in the soft energy band. The most likely explanation for these emission lines is that they are associated with an outflowing gas with a velocity of $\sim 2000 \text{ km/s}$. The data suggest that the same gas which is causing the absorption could also being responsible of these emission features. Finally, the *XMM-Newton* spectrum shows the presence of a relativistic iron emission line likely originated in the accretion disc of a Kerr Black Hole with an inclination of ~ 25 degrees. We propose a model to explain the observed X-ray properties which invokes the presence of a two-phase outflow with cone-like structure and a velocity of the order of 2,000-4,000 km/s. The inner layer of the cone would be less ionised, or even neutral, than the outer layer. The inclination angle of the source would be lower than the opening angle of the outflowing cone.

Key words: galaxies: active – galaxies: nuclei – galaxies: Seyfert – X-rays: galaxies – galaxies: individual: ESO323-G077

1 INTRODUCTION

Fast winds or outflows of ionised gas are known to be common in active galactic nuclei (AGN). They have been detected for the first time in optical/UV spectra. In the X-ray

band, *Asca*, *XMM-Newton* and *Chandra* systematic studies of AGN established that at least half of the active galaxies host warm absorbers (Piconcelli et al. 2005; George et al. 1998; Reynolds & Fabian, 1995; Blustin et al. 2005, Mckernan, Yaqoob & Reynolds, 2007). The evidence of transversal flows (Mathur et al. 1994; Crenshaw et al. 2003, Arav 2004) indicate that they are ubiquitous in AGN, becoming detectable only in certain lines of sight. Typically, the ionised gas has a temperature of $\sim 10^6 \text{ K}$, a density ranging from

^{*} Partially based on observations obtained with XMM-Newton, an ESA science mission with instruments and contributions directly funded by ESA Member States and NASA.
[†] E-mail: elena@astroscu.unam.mx

10^{22} to 10^{23} cm^{-2} , and frequently outflowing with typical velocities of several thousand km/s (Kaspi et al. 2002; Krongold et al. 2003). However, highly ionised absorbers are not so common. Recent studies (e.g. NGC 1365 Risaliti et al. 2005; PG1402+261 Reeves et al. 2004; NGC4051, Krongold et al. 2007; NGC 985 Krongold et al. 2008), show evidence of extreme characteristics of these hot absorbers, as a relativistic velocity of the outflowing gas or a dramatic variability of the absorbing features, indicating that the gas should be located very close to the nucleus of the AGN. Highly ionised absorbers have been probed thanks to the high sensitivity of *XMM-Newton* and *Chandra* in the 2-10 keV. In a recent review, Cappi (2006) reports from the literature a dozen of AGN with blue-shifted Fe absorption lines in their X-ray spectra. However, there are only few cases in which more than one absorption line associated to the same outflowing material is measured. Deep studies of this kind of objects are crucial to establish the presence of these highly ionised absorbers.

According to the paradigm of the origin of AGN, the large energy output of these systems is explained by radiatively efficient accretion onto a supermassive Black Hole. This scenario predicts that the broad relativistic Fe emission line would be a relatively common feature in the X-ray spectrum of AGN. The most outstanding case is MCG-6-30-15 (Tanaka et al. 1995; Wilms et al. 2002, Fabian et al. 2002). However, only about 30% of the objects with proved evidence of the relativistic iron line have been reported (see Nandra et al. 2006 for a recent review, Jiménez-Bailón et al. 2005; Miller et al. 2007). In many cases, the data analysis suggest that highly ionised and highly absorbed material can mimic the spectral characteristic of the relativistically iron line (Reeves et al. 2004). Both, systematic of complete sample studies, as well as accurate determination of the parameters of the broad iron lines based on deep single target analysis, are crucial to understand the physics of the accreting process (Guainazzi et al. 2006, Nandra et al. 2006).

ESO 323-G077 is a nearby ($z=0.015$), bright ($V=13.6$ mag), type I Seyfert galaxy, discovered by Fairall (1992). Winkler (1992) also classified as Seyfert 1 galaxy, although more recently, Veron-Cetty et Veron 2006 classified it as a 1.2 Seyfert galaxy. In X-rays, ESO 323-G077 was detected for the first time in the *Rosat All-Sky Survey*. In the hard band, the galaxy was detected in the *RXTE* Slew Survey (Revnivtsev et al. 2004). The measured luminosity was $L_{3-20 \text{ keV}} \sim 7 \times 10^{42}$ erg/s. The galaxy is also included in the First Integral Catalog (Beckmann et al. 2006), with a luminosity of $L_{2-100 \text{ keV}} \sim 1.6 \times 10^{43}$ erg/s. In this paper we present the results on the analysis of the *XMM-Newton* observation of the Seyfert galaxy ESO 323-G077, which shows evidence of both relativistic iron line and the presence of highly ionised gas in both the X-ray soft and hard band of its spectrum.

2 OBSERVATIONS AND DATA ANALYSIS

The *XMM-Newton* (Jansen et al. 2001) observation of ESO 323-G77 was performed the 7th of February, 2006 (obsid. 0300240501). The *thin* filter and the *large window* mode were selected for the *EPIC* exposures. All *XMM-Newton* data were processed with the standard *Science Analysis System*,

SAS, v7.0.0 (Gabriel et al. 2004) and using the most updated calibration files available in January 2007. The *EPIC* event lists were filtered to ignore periods of high background flaring following the method proposed by Piconcelli et al. (2004). The exposures after background filtering are 24.0, 28.2 and 28.2 ks for *pn*, *MOS1*, and *MOS2*, respectively. According to SAS task *epatplot*, no sign of pile-up was detected in any of the *EPIC* observations. The *RGS* data do not have enough signal-to-noise to perform spectral analysis and therefore they were not considered in the analysis.

The spectra were extracted from circular regions of 35'' and centred on the maximum emission of the source. The background regions were extracted from circular regions of 1' and 1.7' for *pn* and *MOS* observations, respectively. The background regions were selected to be located close to the source and free of any contamination source. After verifying the *MOS1* and *MOS2* agree one with each other, both spectra were combined to obtain a higher signal-to-noise ratio. After background subtraction, both spectra, i.e. the *pn* and the *MOS1-2* combined, were grouped such that each bin contains at least 50 counts per bin. We are therefore able to use the modified χ^2 technique (Kendall et al. 1973) in the spectral analysis. We assumed a flat Λ CDM cosmology with $(\Omega_M, \Omega_\Lambda)=(0.3, 0.7)$ and a value for the Hubble constant of 70 kms^{-1} (Bennett et al. 2003).

2.1 Spectral Analysis

We have performed the spectral analysis of the data using *Xspec* v.12.3 (Arnaud 1996). The *pn* and the combined *MOS* spectra have been fitted simultaneously, leaving to independently vary only the normalisations of the different components. Otherwise indicated, all parameters are given in the ESO 323-G77 rest frame. The errors quoted in this paper refer to the 90% confidence level (i.e. $\Delta\chi^2=2.71$; Avni 1976). For the spectral fitting of the *XMM-Newton* data we have considered the absorption due to the Galaxy, fixing the equivalent Hydrogen column density to $7.4 \times 10^{20} \text{ cm}^{-2}$ (Dickey & Lockman, 1990).

Considering the whole energy band (0.3-10 keV), a power law modified by an intrinsic cold absorption component does not provide an acceptable fit to the *EPIC* data ($\chi^2_\nu \sim 10$). Both positive and negative residuals are clearly present below 3 keV and in the 5–8 keV observed energy band. We therefore ignored the data within these bands and fitted a power law modified with intrinsic absorption. We measured an absorbing equivalent Hydrogen column density of $\sim 6 \times 10^{20} \text{ cm}^{-2}$. The index of the power law resulted to be 1.88 ± 0.05 , in good agreement with typical values of type I AGN (Piconcelli et al. 2005). Figure 1 shows these strong residual after re-notifying the ignored channels. For the sake of clarity, only *pn* data are shown in the plot.

2.1.1 The soft energy band

In order to fit the conspicuous *soft excess*, we reintroduced the energy bins below 3 keV. We then added to the previous model an extra power law emission with the same index of the one associated to the high energy band, as expected for a partial covering scenario. The additional component largely improves the previous fit ($\chi^2_\nu \sim 10$) with a resulting

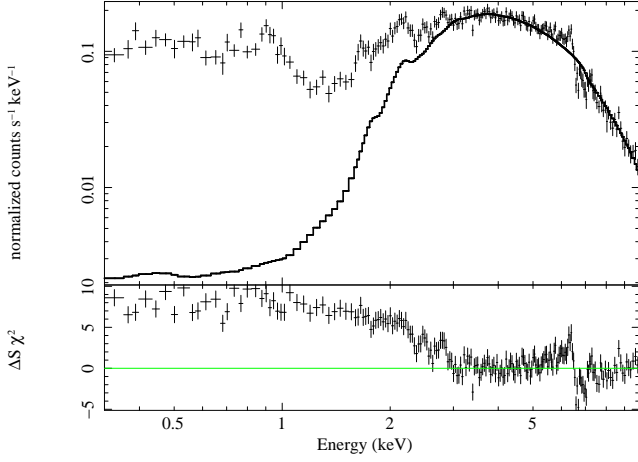


Figure 1. *EPIC-pn* observed spectrum and residuals to an absorbed power law model fitted in the 3–10 keV and ignoring the 5–8 keV band.

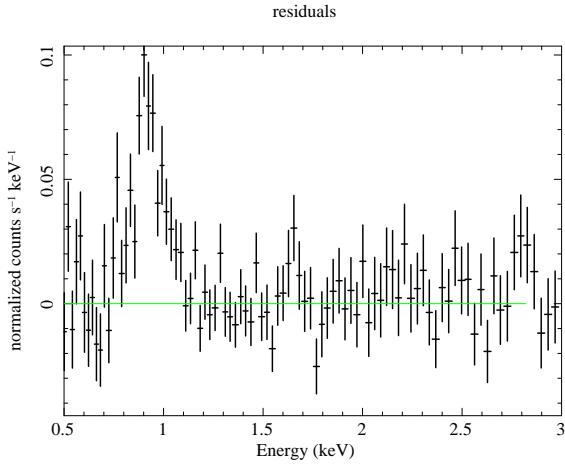


Figure 2. *EPIC-pn* residuals to model A in the 0.5–3 keV band. Emission features are visible at 1 keV, 1.7 keV and 2.8 keV.

χ^2_ν of 1.5. However, this new fit still leaves residuals both in *absorption* and *emission*. We then tested the presence of an extra cold absorption component, located further away from the nucleus and therefore affecting both components (i.e. $wabs*(powerlaw+wabs*powerlaw)$). However, an ionised absorption produced a more adequate fit to the data than the cold one. The warm absorption component has been fitted using the modelisation developed by Krongold et al. 2003, i.e. the *Phase* model. The power law index of the resulting model (i.e. $phase*(powerlaw+wabs*powerlaw)$ labeled as model A in Tables 1 and 2) is $\Gamma = 1.90^{+0.07}_{-0.06}$ and the cold absorption Hydrogen equivalent column $6.34^{+0.18}_{-0.19} \times 10^{22} \text{ cm}^{-2}$. This value is largely higher than typical values of Type-I active galaxies, which are mainly compatible with absorption caused by the host galaxy, i.e. $< 10^{21} \text{ cm}^{-2}$ (Piconcelli et al. 2005). The warm absorber imprinting the soft energy band has a moderately high Hydrogen equivalent column, $n_H = 1.3^{+1.8}_{-0.8} \times 10^{23} \text{ cm}^{-2}$ and an ionization parameter of $\log U = 3.16^{+0.19}_{-0.12}$, where $U = \frac{Q}{4\pi R^2 c n_e}$, Q is the luminosity of the ionising photons, R is the distance to the source and n_e the electron density.

However, further positive residuals are also present

around 1 keV, 1.7 keV and 2.8 keV (see Fig. 2). We have measured two emission lines around ~ 1 keV, (0.93 and 1.04 keV, i.e. 13.3 Å and 11.9 Å, respectively) which could be naturally associated with the NeIX triplet (13.47; 13.55, 13.7 Å) and NeX at 12.13 Å with an outflow velocity of the order of 2,000 km/s. After the inclusion of each of these emission lines, the fit improved at a significant level higher than 99.99%, according to the F-test. Two more emission lines, less significant but still with probabilities of 95.9% and 99.0% are also detected, only in the *pn* spectrum. The measured centroids of the lines are 1.68 keV (7.38 Å) and 2.84 keV (4.37 Å) and could be associated with MgXI (7.85 Å) and SxVI (4.73 Å), respectively. The outflowing velocity of the originating material would be of the order of 20,000 km/s. However, an outflow with a velocity of ~ 2000 km/s would also be possible if lines are identified with other species (see Discussion for further details). The interesting parameters of the lines are given in Table 3.

2.1.2 The hard energy band

Strong and broad positive residuals are visible in the 5–8 keV band. As a first attempt, we fitted them with a single Gaussian line. Considering only the hard band, i.e. 3–10 keV, the χ^2_ν of the fit after the inclusion of the line is still very high, i.e. $\chi^2_\nu = 1.93$ (model B in Table 1). The line energy was measured to be at $6.15^{+0.15}_{-0.13}$ keV and the resulting width of the line of was $0.26^{+0.08}_{-0.04}$ keV, with an equivalent width 200^{+60}_{-20} eV. Figure 3 shows the shape of the residuals to this model between ~ 5 and 7 keV. These results indicate that the spectral feature has a broad and slightly skewed profile. In order to further study the broad emission line, we used the *KYGLine* model for an iron emission line produced from an irradiated disc around a Black Hole developed by Dovčiak, Karas & Yaqoob (2004). This model is parametrised by the energy of the line, the spin of the Black Hole a/M , the inclination of the line of sight with the polar axis of accretion disc, i , and the size of the emission area on the disc, parametrised through the inner and outer radii for non-zero emissivity of the disc relative to the horizon radius, $r_h(a) = 1 + (1 - a^2)^{1/2}$. Regarding to other parameters of the model, we assumed that (i) there is no emission below the last marginal stable orbit, r_{ms} , and the outer radius of the emission ring is $400GM/c^2$; that (ii) the line is emitted from the inner region of the disc with the index of the radial dependence of the emissivity to 3; and that (iii) the disc is emitting isotropically. We also fixed the energy of the line to 6.4 keV, the spin to its maximum value, i.e. $a/M = 0.998$, the outer radius to $400R_g$. We measured an inclination of the disc of 24^{+4}_{-3} deg and an inner radius for the emission from the disc $r_{in} - r_h < 2$. A narrow, neutral emission line with an equivalent width of 37 ± 24 eV is also included in the fit. Both emission lines are statistically significant with levels higher than 99.99%

However, negative residuals are still present in the 6.5–7.5 keV band. These residuals were fitted with two absorption lines with energies of ~ 6.74 keV and ~ 7.1 keV. Both lines resulted to be significant according to the F-test at $\geq 99.99\%$ $\Delta\chi^2 = 50$ and 99.85% $\Delta\chi^2 = 29$ levels, respectively. Contour plot of the line energy versus its intensity for each line are shown in Figure 4.

The equivalent width of the lines are in both cases of the

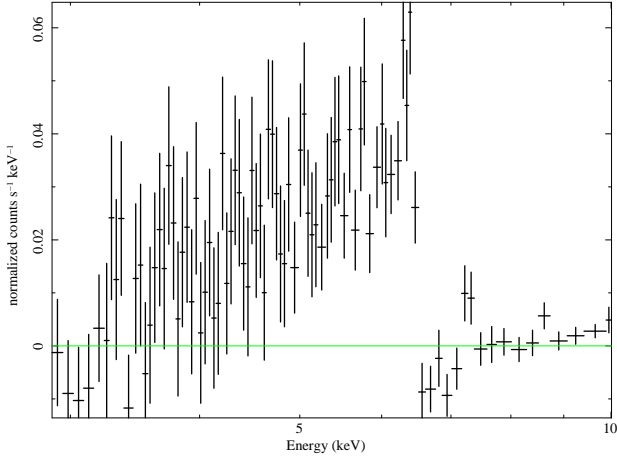


Figure 3. Residuals to a model B consisting of a power law and a Gaussian line fitted in the 3-10 keV band.

order of 50 eV. The energies of these two lines suggest that they are consistent with the Fe XXV and Fe XXVI $K\alpha$ lines. If this is the case, the lines would be blue-shifted with velocities 2000^{+700}_{-1700} and 3000^{+1800}_{-1200} km/s, respectively. These lines should have been originated in a largely ionised material. We therefore used the PHASE model to determine the properties of the absorbing gas (model C in Tables 1 and 2). The absorber is required at a confidence level $>99.99\%$ $\Delta\chi^2 = 5$, according to the F-test. The warm absorber model properly reproduces the absorption features observed in the 6.5–7.5 keV and other weaker lines at higher energies, related to other energy levels of Fe XXVI, that are not statistically significant in a line by line analysis. We measured an equivalent Hydrogen column for the ionised gas of the order of 10^{23} cm^{-2} and an ionisation parameter of $\log U = 3.48^{+0.08}_{-0.11}$. The velocity of the outflowing gas is compatible with the measurements obtained for the absorbing Gaussian lines, $v = 1100^{+1800}_{-400}$ km/s. The large uncertainties are the result of the limited spectral resolution of our data.

2.1.3 The whole energy band

Finally, we modelled the spectrum in the whole energy band. The presence of the broad iron emission line also implies a contribution of the reflected power law by a Compton reflection from a neutral material of the disc. To model this continuum emission we used the *pexrav* model in Xspec (Magdziarz & Zdziarski 1995). The reflection component was relativistically convolved with the intrinsic emissivity from the disc using the *KYConv* model. Therefore, the final best-fit model includes a neutrally absorbed power law plus the reflection component ($R < 0.7$) to account for the continuum emission of the hard energy band; another power law which accounts for the soft band continuum emission, two different warm absorbers, the four emission lines present in the soft energy band and the narrow and broad components of the iron line. The value of the free parameters and goodness of the fit are shown in Tables 1 and 2, labeled as model D. Additionally, the normalisation of the power law associated to the soft energy band is $9.8^{+0.4}_{-0.5} \times 10^{-5}$ photons $\text{keV}^{-1} \text{cm}^{-2} \text{s}^{-1}$ at 1 keV, around 2% of the normalisation value of the hard-band power law, $4.95^{+0.09}_{-0.07} \times 10^{-3}$ photons

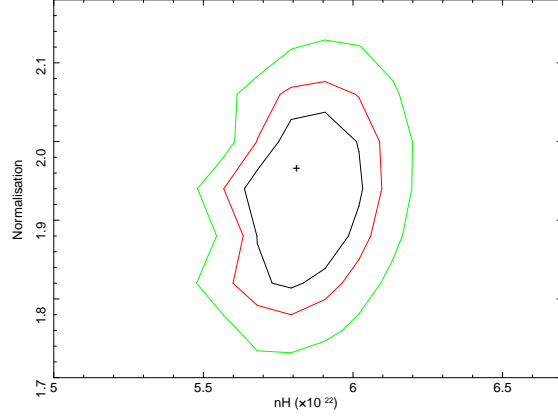


Figure 5. Equivalent Hydrogen column density of the cold absorption component versus the conferring factor contour plot

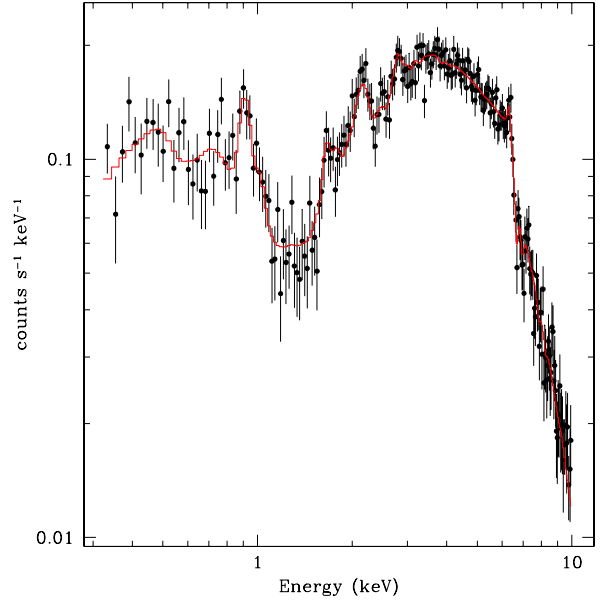


Figure 6. Observed ESO 323-G077 *pn* spectrum and the best fit model.

$\text{keV}^{-1} \text{cm}^{-2} \text{s}^{-1}$ at 1 keV. Figure 5 shows the significance contour levels of the equivalent Hydrogen column density of the cold absorption component versus the covering factor. The best-fit model superimposed to the observed spectrum is shown in Figure 6. We have also checked if the presence of the relativistic iron line is still robust within this model by removing the *KYGline* component: the goodness of the fit worsens significantly, with a value of the $\chi^2 = 624$ for 430 dof.

2.2 Fluxes and luminosities

The derived flux and luminosity, based on the best fit model and referred to the *pn* data, in the 2-10 keV band are $9.9^{+0.2}_{-0.5} \times 10^{-12} \text{ erg cm}^{-2} \text{s}^{-1}$ and $7.5^{+0.2}_{-0.4} \times 10^{42} \text{ erg/s}$, re-

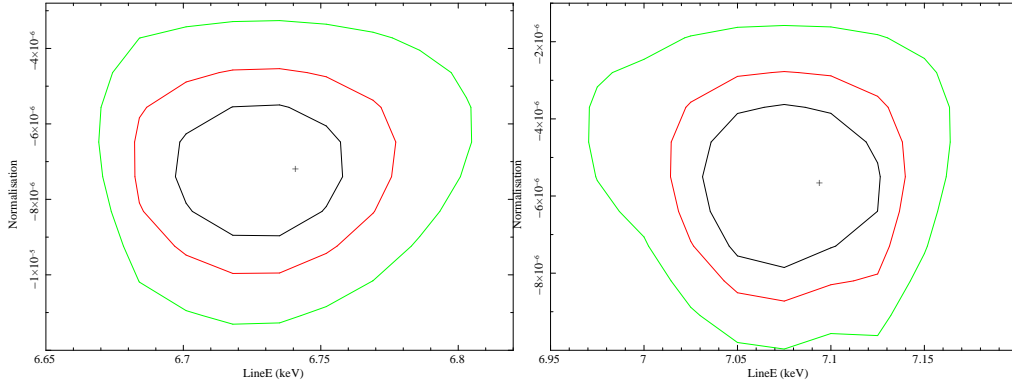


Figure 4. Line energy versus intensity contour plots for both high energy absorption lines located at ~ 6.74 keV and ~ 7.1 keV, left and right panel, respectively.

Table 1. Values of the parameters and goodness of the fits of the different models applied to the *EPIC* spectra of ESO 322-G077. WA indicates warm absorption component.

Model	PowerLaw Γ	Cold Absorption n_H 10^{22}cm^{-2}	WA <i>Low</i> <i>ionisation</i>	WA <i>High</i> <i>ionisation</i>	E keV	σ keV	Broad Iron Line i/EW deg/eV	rin-rh	a/M	Goodness χ	DOF
A	$1.90^{+0.07}_{-0.06}$	$6.34^{+0.18}_{-0.17}$	✓							413	285
B	$2.33^{+0.10}_{-0.09}$	$8.7^{+1.2}_{-1.0}$			$6.15^{+0.15}_{-0.13}$	$0.26^{+0.08}_{-0.04}$	200^{+60}_{-20}			339	216
C	$1.95^{+0.03}_{-0.04}$	$6.28^{+0.14}_{-0.17}$	✓		6.4f	-	24^{+4}_{-3}	< 2.0	0.9982f	544	439
D	1.99 ± 0.02	$5.82^{+0.12}_{-0.11}$	✓	✓	6.4f	-	26^{+2}_{-4}	< 1.6	0.9982f	407	424
D [†]	1.99 ± 0.02	$5.82^{+0.10}_{-0.13}$	✓	✓	6.4f	-	26^{+3}_{-4}	< 1.3	> 0.86	406	423

Table 3. Soft energy band emission lines energy, equivalent widths, fluxes, and significance according to the F-test.

Energy keV	EW eV	Flux $10^{-15} \text{erg cm}^{-2} \text{s}^{-1}$	F-test	$\Delta\chi^2$
0.93	190^{+120}_{-20}	18^{+4}_{-2}	$> 99.99\%$	190
1.04	59^{+15}_{-16}	3^{+3}_{-2}	$> 99.99\%$	25
1.68	36^{+13}_{-14}	< 6	95.9%	6
2.84	18^{+9}_{-6}	22^{+11}_{-19}	99.0%	9

spectively. In the soft band, the corresponding flux and luminosity are 0.5-2 keV, $(2.3^{+0.5}_{-0.4}) \times 10^{-13} \text{erg cm}^{-2} \text{s}^{-1}$ and $(5.1^{+1.1}_{-1.0}) \times 10^{42} \text{erg/s}$.

We investigated a possible short-term variability of the source, i.e. within the observation. We used the *clean pn* events to derive the light-curves in different energy bands. There is no clear sign of variability within the observation, neither in the soft nor in the hard band. Only *RXTE* and *Integral* previously observed the source in the hard band. ESO323-G077 is included in the serendipitous survey of *RXTE* obtained during satellite re-orientations (Revnivtsev et al. 2004) during the 1996-2002 period. However, the observation date is not specified in the catalogue. Based on the flux measurements performed by Sazonov & Revnivtsev (2004), we calculated a 2-10 keV flux of $\sim 9 \times 10^{-12} \text{erg cm}^{-2} \text{s}^{-1}$. Similar result is obtained when *Integral* luminosity is considered. Therefore, no short or long-term variability can be deduced from the present data.

3 DISCUSSION

3.1 The origin of the soft excess

Figure 1 shows the conspicuous *soft excess* of ESO 323-G77. The origin of this feature in Type-I objects is still an open issue. In general, the shape of the *soft excess* can be fitted by a thermal component, i.e. black-body, bremsstrahlung emission. However, the temperatures measured for large variety of AGN (i.e. with different intrinsic luminosities, Black Hole masses, accretion rates...) are of the same order of magnitude (Piconcelli et al. 2005). This result is difficult to explain in any scenario related to a continuum emission from an accretion disc. A probably more realistic scenario explains the soft excess emission due to absorption or emission processes, associated to atomic transitions seen blurred to relativistic effects (Gierliński & Done, 2004, Crummy et al. 2006; Schurch & Done, 2006). Although, the origin of the *soft excess* of ESO 323-G77 is out of the scope of the paper some different scenarios are discussed. In particular, fits using thermal models (i.e. *blackbody*, *bremsstrahlung*,...) to resemble the soft excess statistically failed. A power law accounting for the soft excess provided good results, as showed in previous section, i.e. the partial covering scenario. The typical scenarios for Seyfert 1 galaxies described above is not plausible due to the presence of the cold absorber, which according to these modelisations should be placed close to the *soft excess* emission source, i.e. the accretion disc, yielding therefore a very unlikely scenario. Within the partial covering approach, we checked the robustness of the hypothesis by leaving free to vary the soft band power law index. We find a very good

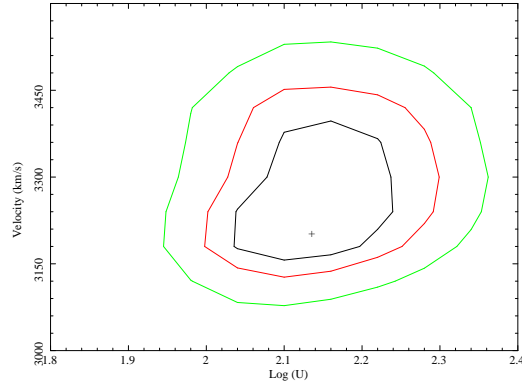
Table 2. Values of the parameters of the warm absorption components and goodness of the fits of the different models applied to the *EPIC* spectra of ESO 322-G077.

Model	Low Ionised Warm Absorption				High Ionised Warm Absorption				Goodness	
	n_H (10^{22}cm^{-2})	$\log U$	$v_{turb}(\text{km/s})$	$v(\text{km/s})$	n_H (10^{22}cm^{-2})	$\log U$	$v_{turb}(\text{km/s})$	$v(\text{km/s})$	χ	DOF
A	13^{+18}_{-8}	$3.16^{+0.19}_{-0.12}$	300f	< 3600					413	285
C	9^{+5}_{-3}	$3.48^{+0.08}_{-0.11}$	300f	1100^{+1800}_{-400}					544	439
D	$1.9^{+0.4}_{-0.3}$	$2.14^{+0.06}_{-0.07}$	< 140	3200^{+600}_{-200}	13^{+8}_{-4}	$3.26^{+0.19}_{-0.15}$	500 ± 400	1700^{+600}_{-400}	407	424
D†	$1.9^{+0.4}_{-0.3}$	2.14 ± 0.06	< 140	3200^{+600}_{-300}	13^{+8}_{-4}	$3.23^{+0.18}_{-0.14}$	500^{+400}_{-300}	1600^{+600}_{-300}	406	423

agreement, $\Gamma_s = 2.03^{+0.13}_{-0.12}$ versus $\Gamma_s = 1.99 \pm 0.02$, between both indexes. Moreover, the strength of the secondary component is only 2% of the primary: a low fraction of the normalisation expected for this scenario. If instead, the power law emission is placed outside the absorbing components (both the neutral and the ionised ones), the fit is statistical indistinguishable to our best-fit model. The resulting index is 2.29 ± 0.09 , in agreement with typical values of Type-I objects (Piconcelli et al. 2005). However, this model is only phenomenological, as it does not correspond to any obvious physical scenario.

Alternatively, the *soft excess* observed in *ESO 323-G77* could also be related to the emission/reflection of an ionised plasma, as observed in many Seyfert 2 objects. This scenario has been studied using high resolution X-ray spectra for individual objects (e.g. NGC1068, Kinkhabwala et al. 2002; Circinus, Sambruna et al. 2001; Mrk3, Bianchi et al. 2005) and for sample of objects (Bianchi et al. 2006). Bianchi et al. (2006) find that the *soft excess* is nearly ubiquitous in Seyfert 2. Based on their high resolution X-ray spectral analysis, the authors claim that the main contribution to the *soft excess* is photoionised emission of extended circumnuclear gas, illuminated by the AGN itself. The soft spectra of Seyfert 2 are dominated by emission lines of highly ionised elements and narrow radiative recombination continua features associated to plasma emission of temperatures of few eV. In their sample, only three out of ten of the studied sources present luminosities higher than 10^{41} erg/s. In *ESO 323-G77*, the *soft excess* associated luminosity measured is of the order of 1.5×10^{41} erg/s. If its *soft excess* is caused by the ionised plasma, the emission lines and the radiative continua would have been visible in the RGS spectra. Therefore, although this scenario is somehow plausible on spectral modeling basis, the large luminosity measured in our source makes this origin unlikely. Finally, an alternative origin for the *soft excess* is the emission from collisionally-ionised plasma. Interestingly, for the largely studied Seyfert 2 galaxy NGC 1068, the contribution of such an emission is constrained to be less than 10% (Brinkman et al. 2002). Additionally, and as in the hypothesis of the photoionised plasma as the explanation of the *soft excess*, the lack of detection of emission lines in the high resolution spectrograph allow us to reject this possibility. A contribution of possible circumnuclear star-forming regions on *ESO 323-G77*, can be ruled out due also to the large luminosity measured.

In summary, in the case of *ESO 323-G77*, the lack of high resolution X-ray data prevents us from deriving any firm conclusion on the origin of the *soft excess* of our source,

**Figure 7.** Contour plots of the velocity of the outflowing gas versus ionisation parameter of the low ionised absorber.

leaving as the most probable origin the partial covering scenario with only a possible minor contribution of emission/reflection of ionised plasma.

3.2 The ionised absorbers and emitter

Both in the soft and the hard X-ray spectrum of ESO 323-G077, several absorption features are present. In Section 2, we reported the presence of two different warm absorbers which partially explain the noticeable absorption features in the spectrum.

The low ionised absorber

Warm absorbers are quite common in Seyfert 1 galaxies. Around 50% of these systems present absorbing features originated by ionised material. The less ionised absorber detected in *ESO 323-G77* has an ionisation parameter of $2.14^{+0.06}_{-0.07}$ with an associated temperature of 6.9×10^5 K, an equivalent Hydrogen column of $1.9^{+0.4}_{-0.3} \times 10^{22} \text{cm}^{-2}$ and a turbulent velocity < 140 km/s. The spectral analysis does not allow to constrain the turbulent velocity as no absorption lines were resolved in the *EPIC* spectrum. The fit reveals that the absorption takes place in an outflowing gas with velocities between 2800 and 3400 km/s. Fig. 7 shows the contour plot of the velocity of the outflowing gas versus the ionisation parameter. The lack of high resolution spectra with enough signal-to-noise ratio, prevents us from determining more accurately the outflowing gas velocity. In the upper panel of Fig. 8, the imprints of this absorber are shown. The absorption is mainly affecting the low energy band, i.e. < 2 keV, but it is also affecting the Fe energy band.

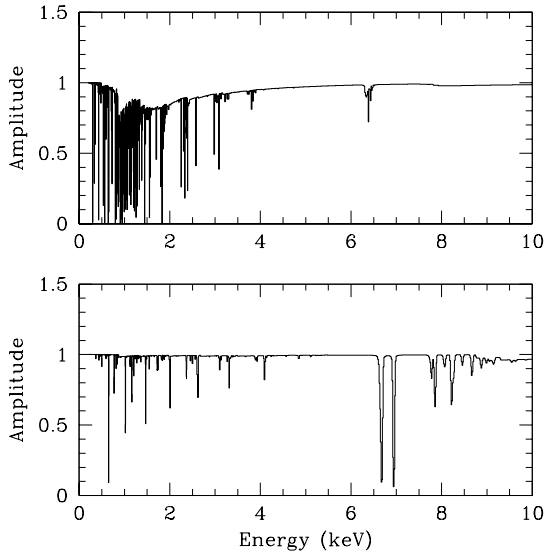


Figure 8. Modelisation of the warm absorption features of the low (upper panel) and high (lower panel) ionised absorbers.

The high ionised absorber

Recently, the high spectral resolution and sensitivity of *XMM-Newton* and *Chandra* allow the study of highly ionised absorbers in AGN which imprint on the high X-ray energy spectra. Even if less common than the moderately and low ionised absorbers, these more extreme absorbers have been reported for several objects (e.g. PG1211+143, Pounds & Reeves, 2007, Reeves et al. 2008; PG2112+059, Schartel et al. 2005, 2007; NGC1365, Risaliti et al. 2005; PG1402+261, Reeves et al. 2004; PG1001+054, Schartel et al 2005; PG1535+547, Schartel et al 2005) *ESO 323-G77* unambiguously hosts a high ionised absorber. In the hard band, two absorption lines, associated with FeXXV and FeXXVI, are observed at a confidence level higher than 99.9%. The measured energies of the lines indicate that they are blue-shifted with associated velocities of the order of 2000-3000 km/s. We have also reproduced them using the warm absorber code *phase*. The ionisation parameter resulted to be $3.26^{+0.19}_{-0.15}$ with an associated temperature of 2.7×10^6 K and the measured equivalent column density $13^{+8}_{-4} \times 10^{22} \text{ cm}^{-2}$. A global fit to both lines allowed a more accurate measurement of the velocity of the gas, $v = 1700^{+600}_{-400} \text{ km/s}$. The parameters of the warm absorber could have been accurately determined because of the presence of the two absorption lines which have been modelled jointly. The lower panel of Fig. 8 shows this absorber. The properties of the highly ionised absorbing gas are therefore not as extreme as the ones reported for other AGN, (e.g. PG0844+349): the measured velocity of the gas does not required to invoke relativistic effects as its value is similar to those of typical warm absorbers. The equivalent Hydrogen absorbing column measured is also in the range of common values and finally no evidence of rapid variability has been detected. However, the accurate determination of the properties of the highly ionised absorbing gas through the *Phase* model allows us to more firmly establish the presence of the broad relativistic iron emission line in ESO323-G077. Al-

though high energy (i.e. $\sim 7 - 10 \text{ keV}$) absorption lines have been detected in a dozen of objects (see Cappi et al. 2006 for a recent review), it is not common to observe several of these lines for the same object. Moreover, for several of these objects in which more than one of these absorption line are detected in their spectra (PDS 456, Reeves et al. 2003; PG1115+080, Chartas et al. 2003; APM08279+52551, Chartas et al. 2002, Hasinger et al. 2002), the analysis revealed that they are associated to warm absorbers with different properties (i.e. velocity, ionisation parameter...). Therefore, the case of *ESO 323-G77* is very interesting as the presence of its highly ionised absorber is more robust as it is probed by more than one line. This finding for *ESO 323-G77* is very similar to the case of MCG-6-30-15, for which an outflow with $\log \xi = 3.6$ and $v \sim 2000 \text{ km/s}$ is generating two absorption lines associated to $K\alpha$ lines of FeXXV and FeXXVI (Young et al. 2005). The best example is, however, the case of NGC1365 (Risaliti et al. 2005), where four lines associated with $K\alpha$ and $K\beta$ states of both FeXXV and FeXXVI were detected (see also, Netzer et al. 2003 for NGC3783 and Steenbrugge et al 2005 for NGC 5548).

The ionised emitter

Four emission lines have been detected in the soft energy band with confidence levels $> 95\%$, see Figure 2 . The centroid energy of the lines have not been well determined due to the limited statistics, and therefore, no uncertainties in the energy line could have been given. However, based only on the best-fit values, we have associated each detected line to the most likely specie. The most prominent line is located at $\sim 0.93 \text{ keV}$ (13.3\AA). We have identified it with the NeIX triplet, as it is the most prominent one in this spectral region. If this is the case, the observed line would have been blueshifted with a velocity of $\sim 2,000\text{-}4,000 \text{ km/s}$, depending on which line of the triplet we considered. Another intense emission line, FeXIX $\lambda 13.52\text{\AA}$, may also be contributing to the observed emission and would also be originated in the same media. The second more significant line, located at 1.04 keV (11.9\AA), is very likely originated by NeX $\lambda 12.13\text{\AA}$. The outflowing gas which is originating this line would be the same which is responsible for the line at $\sim 0.93 \text{ keV}$, as the blueshifted velocity is also of the order of $2,000 \text{ km/s}$. The line detected at 1.68 keV (7.38\AA) is also compatible with being originated in an outflowing gas of $\sim 2,000 \text{ km/s}$ and would be associated with FeXXIII $\lambda 7.48\text{\AA}$. However, a more intense line is located at 7.85\AA (Mg XI), but the outflowing velocity of the gas would be of the order of $20,000 \text{ km/s}$. Finally, the line detected at 2.84 keV (4.37\AA) can be associated with S XVI $\lambda 4.73\text{\AA}$, which is the only close known emission line. However, in this case, the outflowing velocity of the gas would be $\sim 20,000 \text{ km/s}$. Alternatively, Kaspi et al. (2002) detected in the high resolution spectrum of NGC3783 an unidentified emission line at 4.35\AA . In our case, this line could be originated in the same outflowing material with a velocity of $2,000 \text{ km/s}$. In summary, the most prominent lines detected in the *ESO 323-G77* spectrum are likely associated with NeIX (with a possible contribution of FeXIX) and NeX. The emitting media would be outflowing with a velocity of $\sim 2,000 \text{ km/s}$. This value is compatible with the velocity measured for the outflowing material which is causing the highly ionised absorption. Therefore, it is likely that the same material which is absorbing the primary emission

is also responsible of the emission. Although it is possible that the same gas is also originating the other two emission lines, it is necessary to force the identifications of the detected lines with rare species. On the other hand, if these emission lines are identified with the most probable lines, i.e. Mg XI and S XVI, then the velocity of the outflowing gas is abnormally high, (20,000 km/s). Moreover, the abundance deduced if these are actually the correct identifications would be also abnormal, with largely sub-solar abundances of Iron, Oxygen, Silicon and Nitrogen. Therefore, the fact that the velocities calculated through the line identification are compatible one with the other reinforces the hypothesis of the high speed wind. It is, however, worth noting that the lines with higher energy are less significant, and therefore no firm conclusions can be reached with our data.

Besides this, it is surprising that the strongest emission line detected is associated with the Ne IX triplet, but no hint of O VII is detected in the spectrum. A possible explanation is that the metallicity of the gas is largely different from the solar one. Super-solar metallicities have been measured in Narrow Line Seyfert 1 (NLS1). In fact, the same features observed in *ESO 323-G77* (i.e. Ne IX emission line with absence of Oxygen lines) has also been detected in Mrk 1239 (Grupe, Mathur & Komossa, 2004). A similar example of super-solar abundance was measured in X-rays for Mrk 1044 (Fields et al. 2005; see also Shemmer & Netzer, 2002). However, although super-solar metallicities are common among NLS1, there is only one previous example of super-solar abundance in a Seyfert 1 galaxy, Mrk 279 (Fields et al. 2007). Our result is very interesting in the framework of the enrichment of the intergalactic medium (Williams et al. 2005), as a similar trend is observed in the O/Ne ratio. The amount of mass ejected for *ESO 323-G77* in the media is not negligible. The mass outflow rate depends on the distance of the warm absorber from the source, the column density, the radial velocity of the outflow, the angle of the line of sight and the angle between the accretion disc and the gas flow. We can assume an angle of the line of sight of $\sim 40^\circ$ and an angle of the outflow of $\sim 60^\circ$.

The location of the ionised gas in *ESO 323-G77* could not be determined, however, an order of magnitude of this quantity can be estimated assuming that it correlates with the square root of the bolometric luminosity. Krongold et al. (2007) calculated accurately the location of the warm absorber of NGC 4051 at 0.1 lt-days from the nucleus. For *ESO 323-G77*, we estimated the bolometric luminosity using the correlation given by Elvis et al. 1994, $L_{bol}^{ESO} \sim (2 - 4) \times 10^{44}$ erg/s. Taking into account this measurement and scaling it with luminosity of NGC 4051, the outflowing gas in *ESO 323-G77* would be located at 1.5-3 lt-days. We therefore estimate the mass outflow ratio to be of the order $1.2 \times 10^{-2} M_\odot/\text{yr}$. This corresponds to a kinetic energy of $\sim 3 \times 10^{40}$ erg/s, which compared with the bolometric energy of the galaxy, corresponds to a fraction of accretion energy of the order of 10^{-4} . Considering a lifetime of 10^8 years for the AGN, it corresponds to a total mass ejected in the media of the order of $1.5 \times 10^6 M_\odot$. The corresponding kinetic energy (considering the outflow velocity of 2000 km/s) would be $\sim 10^{55}$ erg/s. This value is large enough to disrupt the interstellar medium, causing an overabundance (see Krongold et al. 2007 for further discussion).

3.3 The broad Iron emission line

The *XMM-Newton* hard band spectrum of ESO323-G077 reveals that the emission is complex. The most prominent feature in the hard band is a relativistically broaden emission iron line. According to the last studies based on *XMM-Newton* and *Chandra* data, the occurrence of relativistic broad iron emission lines in AGN is rare (Fabian & Miniutti, 2005; Jiménez-Bailón et al. 2005). Although it is also worth noting that recent results based on analysis of a large sample of AGN with enough signal-to-noise in the hard X-ray band show that relativistically broadened Fe K α lines are indeed common. Guainazzi et al. 2006 (but see also Longinotti et al. 2007 and Nandra et al. 2007) detected broad iron lines in 25-50% of the objects. Nandra et al. 2007 also finds an occurrence of relativistic broaden Fe line in 30-45% of a sample of Seyfert 1 and intermediate type of AGN. However, the actual fraction is a matter of debate.

One important issue is the fact that a highly ionised absorption can mimic the features of a relativistic iron line, see for example the case of PG1402+262 (Reeves et al. 2004), evidenced the importance of an accurate fit of the data. The imprints of a highly ionised absorbing component in the X-ray spectrum of *ESO 323-G77* are prominent. At least two absorption lines associated to the K α states of FeXXV and FeXXVI are clearly visible in the spectrum. We found that a dense, $n_H \sim 10^{23} \text{ cm}^{-2}$, ionised ($\log U \sim 3.5$) absorber is responsible for the lines. Besides that, systematic studies of X-ray emission of AGN show that the neutral and narrow Fe emission line is nearly ubiquitous, (Jiménez-Bailón et al. 2005; Bianchi et al. 2004). In our analysis, both the narrow component of the iron and the ionised absorption have been taken into account and the presence of the broad iron line is robust. Figure 9 shows a comparison of the best fits for the modelisation with and without the presence of a broad iron line. The figure also shows graphically the strength and significance of the line.

The complexity of the emission in the hard band and the quality of the present *XMM-Newton* spectral data do not allow us to investigate in great detail the parameters of the broad emission line. However, the analysis indicates that the broad emission line detected in *ESO 323-G77* is one of the most prominent ones observed so far. The EW of the line, when a broad Gaussian line is fitted, resulted to be 200^{+60}_{-20} eV. This value is higher than the mean EW of a local sample of Seyfert 1 galaxies, $\langle EW \rangle = 91 \pm 13$ eV (Nandra et al. 2007), but comparable to the values of relativistically broaden Fe lines (e.g. EW(NGC3516)= 394^{+72}_{-63} eV Nandra et al. (2007); EW(MGC-6-30-15)= 198^{+33}_{-30} eV Nandra et al. (2007); EW(4U1344-60)= 393^{+122}_{-107} eV Piconcelli et al. 2006; Jiménez-Bailón et al. 2006); see other examples in Nandra et al. 2007). When the *KYGline* model is considered, the EW measured resulted to be 450^{+15}_{-110} eV. This value is slightly higher, but of the same order of magnitude than the EW measured for the prototypical MGC-6-30-15 using the same model, ($\sim 270 \pm 10$ eV, Dovčiak, Karas & Yaqoob, 2004). We have investigated the possibility of an overabundance of iron to explain the strength of the measured line. The effect of the iron abundance is clearly imprinted in the strength of the Compton reflection hump. Unfortunately, the lack of data above 10 keV prevents us from investigating in detailed this parameter. The *XMM-Newton* spectral analysis allows

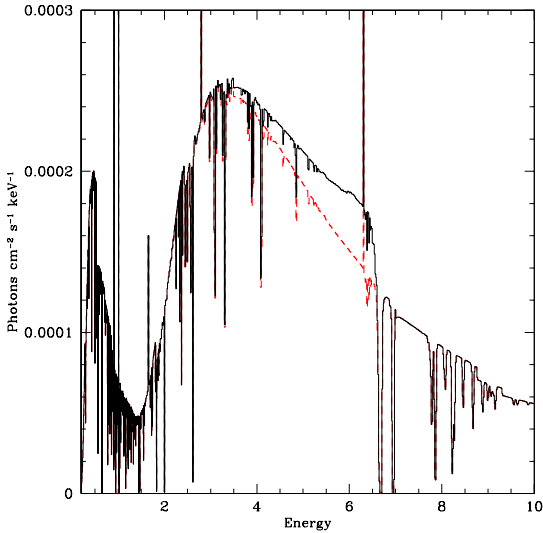


Figure 9. Best fit model of *ESO 323-G077* in solid line and fitted model excluding the relativistically broad emission line component in dashed line.

us to derived only an upper limit of 0.7 for the reflection parameter ($R=\Omega/2\pi$). Although this value is not indicative as we lack the higher energy spectrum of the source, it is in good agreement with the results for a sample of ten Seyfert 1 galaxies performed with *Beppo-SAX* (Perola et al. 2002). If we considered only the five objects in the samples which according to Nandra et al. (2007) host a relativistically broaden iron line, the R parameter ranges from 0.25 to 1.65 and its mean value is 0.7. Similarly, the abundance of iron is not well constrained in our analysis, $A_{Fe} = 2.4^{+7.3}_{-1.9}$ times the solar value. The fit hints, however, an overabundance of iron, ~ 2.5 solar times. This also the case of MGC-6-30-15 (Miniutti et al. 2007), where the abundance of iron is $2.0^{+1.4}_{-0.6}$ solar times. According to our best fit model, the line should be originated in a rotating black hole with an inclination of around 25 degrees. Nandra et al. (2007) showed that the mean value of the inclination of the accretion disc measured for their sample is 36 ± 6 degrees, in fairly good agreement with our results. Furthermore, we have calculated the confidence of these two parameters, together with the innermost stable radius. Figure 10a shows the one, two and three σ contour plot of the inclination of the accretion disc and the inner radius for the stable emissivity. We have also let the spin parameter free to vary, but fixing the inner radius of the emitting ring to be at the horizon radius. This fit presents indistinguishable χ^2 values with respect to the one found for model D and compatible values of the interesting parameters. The values of the parameters and goodness of the fit are given in tables 1 and 2, labeled as model D[†]. The measured spin of the black hole resulted to be > 0.86 . The confidence contours of the spin of the black hole and the inclination of the accretion disc are shown in Fig 10b. Finally, we have checked the stability of the index of the emissivity law. The fit of model D, once this parameter is left free, does not improve significantly. The measured index of the emissivity law was $3.2^{+0.3}_{-0.4}$. The contours plots of this parameter

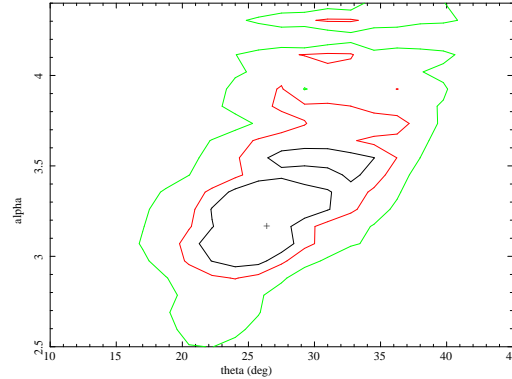


Figure 11. Emissivity index versus accretion disc inclination contour plot using model D.

with the inclination of the disc have been shown in Fig 11. These fits show that despite the degeneracy among the parameters, the relativistic emission lines remains significant in all cases.

3.4 Possible physical interpretation

The *XMM-Newton* X-ray spectrum of *ESO 323-G077* reveals a complex emission. We have detected the imprints of cold absorption with an equivalent Hydrogen column uncommonly high for Type-I objects. Two warm absorbers with different absorption columns and ionisation degrees but with compatible outflowing velocities have been also detected, as in other objects (NGC985 Krongold et al. 2008; NGC 4051 Krongold et al. 2005; NGC3783 Krongold et al. 2003). Several blue-shifted emission lines with velocities compatible with the one measured for the warm absorbers are also imprinted in the *ESO 323-G077* X-ray spectrum. Besides that, the X-ray analysis evidences the robust presence of a relativistically broaden iron line. One plausible physical scenario which explains the observed X-ray properties invokes a two-phase gas in a conical shape outflowing along the polar axis (see Elvis 2000; Krongold et al. 2007). In our case, the outer layer of the conical outflow would be ionised, while the innermost layer would be much less ionised or even neutral. This can be obtained if a large gradient for the electron density occurs along the transversal axis of the cone. The line of sight should be such that allows to observe in the X-ray spectrum the imprints of the warm absorbers and the emitter with the measured outflowing velocity. An inclination angle higher than the opening angle of the optically thick obscuring material invoked in UM and lower than the opening angle of the cone is required to explain both the properties of the warm absorption/emission and the presence of the broad iron lines. This estimation is also compatible with results based on studies in polarised light (Schmid, Appenzeller & Burch, 2003), in which the inclination angle calculated is close to 45° . Interestingly, the polarised light is roughly perpendicular to the [OIII] extended emission (Mulchaey et al. 1996) suggesting that the ionisation cones (normally associated to the [OIII] emission) are responsible of the polarisation. The two warm absorbers fitted to the spectrum suggests that either the outflowing absorber has only two differentiated phases or a continuum degree of ionisation but only two components could have been mod-

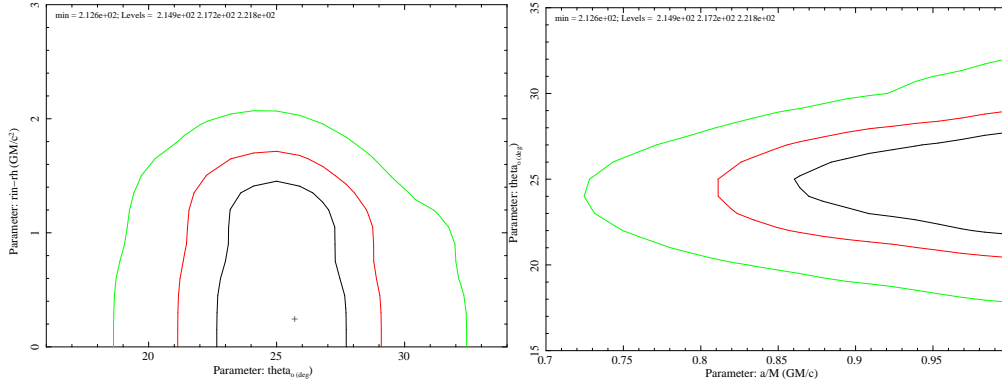


Figure 10. Inclination of the disc versus rin-rh (left panel) and Black Hole spin (right panel) contour plots using model D.

eled. This geometry also explains the emission lines observed with the same blue-shifted luminosity. The innermost neutral layer is evidenced by the neutral absorption measured. At the same time, this component is also blocking the red-shifted emission associated to the opposite side of the cone, explaining why only the blue-shifted component in the emitter is observed.

4 CONCLUSIONS

We reported the results on the analysis of the X-ray spectral emission of the Seyfert 1 galaxy *ESO 323-G77*. The *XMM-Newton* data of the source reveal a complex spectrum with prominent absorption and emission features. The continuum emission can be explained with a power law with an index roughly similar to those of Seyfert 1 galaxies, $\Gamma = 1.99 \pm 0.02$. On the contrary, the cold absorption ($n_H = 5.85^{+0.12}_{-0.11} \times 10^{22} \text{ cm}^{-2}$) is large if compared with common values of type I objects. In addition, two warm absorption components have been also detected in the spectrum. The less ionised absorbing gas with $\log U = 2.14^{+0.06}_{-0.07}$ and an equivalent Hydrogen column of $1.9^{+0.4}_{-0.3} \times 10^{22} \text{ cm}^{-2}$ was measured to be outflowing with a velocity in the 2,000-3,000 km/s range. The high ionised absorber, ($\log U = 3.26^{+0.19}_{-0.15}$ and $n_H = 13^{+8}_{-4} \times 10^{22} \text{ cm}^{-2}$) presents a lower outflowing velocity, $v = 1700^{+600}_{-400} \text{ km/s}$. A series of four emission lines have been detected in the soft energy band. The two most prominent ones are likely associated to the Ne IX triplet (with a probable contribution of Fe XIX) and to Ne X. If this is the case, the associated outflowing velocities would be of the order of 2,000-4,000 km/s. Therefore, the material which is causing the absorption can also be responsible of the emission features detected. The fact that the strongest emission line detected is the one associated with Ne IX while no hint of O VII is detected in the X-ray spectrum indicates that the metallicity is largely different from the solar one. This result has interesting implications to explain the metallicity of the interstellar medium if AGN play an important role in the feedback. The other two emission lines, less statistically significant, can be identified with Mg XI and S XVI, and hence being emitted by an outflowing gas with extreme velocity of $\sim 20,000 \text{ km/s}$, implying also uncommon abundance. An outflowing gas with a velocity of 2,000 km/s would relate one of the lines with an unidentified transition. However, the low statistics of the spectrum in this region does not

allow us to reach firm conclusions. Interestingly, apart from the narrow Iron emission line a broad component has been also detected in the *ESO 323-G77* spectrum. The analysis shows that the presence of this line is robust and it is compatible with being originated in the accretion disc of a rotating Black Hole with an inclination of around 25° . A plausible physical model for this source consists of a two-phase outflowing gas with cone-like structure originated in the inner region of the AGN with a velocity of the order of 2,000-4,000 km/s. The inner layer would be less ionised (or even neutral) than the outer one in order to reproduced the observed X-ray properties. The system would be observed with an inclination angle higher than the opening angle of the obscuring material invoked in UM and lower than the angle subtended by the cone. This scenario is roughly compatible with the results from the relativistic iron line and with the studies of the sources in polarised light in which an inclination angle of 45° is addressed.

ACKNOWLEDGEMENTS

The authors kindly thank the anonymous referee for the useful comments and suggestions that significantly improved the paper. We also thank Matteo Guainazzi for very useful discussions. EJB and YK acknowledge support from the Faculty of the European Space Astronomy Centre (ESAC) and warmly thank the hospitality of the XMM-Newton Science Operation Center.

REFERENCES

- Arav N., 2004, ASPC, 311, 213
- Arnaud, K. A., 1996, ASP Conf.Ser. Vol. 101, Astronomical Data Analysis and Systems, 17
- Avni, Y. 1976, ApJ, 210, 642
- Beckmann V., Gehrels N., Shrader C. R., Soldi S., 2006, ApJ, 638, 642
- Bennett, C. L., et al. 2003, ApJS, 148, 1
- Bianchi S., Guainazzi M., Chiaiberge M., 2006, A&A, 448, 499
- Bianchi S., Miniutti G., Fabian A. C., Iwasawa K., 2005, MNRAS, 360, 380
- Bianchi S., Matt G., Balestra I., Guainazzi M., Perola G. C., 2004, A&A, 422, 65

- Blustin, A. J., Page, M. J., Fuerst, S. V., Branduardi-Raymont, G., & Ashton, C. E. 2005, *A&A*, 431, 111
- Brinkman A. C., Kaastra J. S., van der Meer R. L. J., Kinkhabwala A., Behar E., Kahn S. M., Paerels F. B. S., Sako M., 2002, *A&A*, 396, 761
- Cappi M., 2006, *AN*, 327, 1012
- Chartas G., Brandt W. N., Gallagher S. C., 2003, *ApJ*, 595, 85
- Chartas G., Brandt W. N., Gallagher S. C., Garmire G. P., 2002, *ApJ*, 579, 169
- Crenshaw D. M., Kraemer S. B., George I. M., 2003, *ARA&A*, 41, 117
- Crummy J., Fabian A. C., Gallo L., Ross R. R., 2006, *MNRAS*, 365, 1067
- Dickey, J. M., & Lockman, F. J. 1990, *ARA&A*, 28, 215
- Dovčiak M., Karas V., Yaqoob T., 2004, *ApJS*, 153, 205
- Elvis M., 2000, *ApJ*, 545, 63
- Elvis M., et al., 1994, *ApJS*, 95, 1
- Fabian A. C., Miniutti G., 2005, *astro*, arXiv:astro-ph/0507409
- Fabian A. C., et al., 2002, *MNRAS*, 335, L1
- Fairall A. P., et al., 1992, *AJ*, 103, 11
- Fields D. L., Mathur S., Krongold Y., Williams R., Nicastro F., 2007, *ApJ*, 666, 828
- Fields D. L., Mathur S., Pogge R. W., Nicastro F., Komossa S., Krongold Y., 2005, *ApJ*, 634, 928
- Gabriel, C., et al. 2004, *ASP Conf. Ser.* 314: *Astronomical Data Analysis Software and Systems (ADASS) XIII*, 314, 759
- George, I. M., Turner, T. J., Netzer, H., Nandra, K., Mushotzky, R. F., & Yaqoob, T. 1998, *ApJS*, 114, 73
- Gierliński M., Done C., 2004, *MNRAS*, 349, L7
- Guainazzi M., Bianchi S., Dovčiak M., 2006, *AN*, 327, 1032
- Grupe D., Mathur S., Komossa S., 2004, *AJ*, 127, 3161
- Hasinger G., Scharrel N., Komossa S., 2002, *ApJ*, 573, L77
- Jansen F., Lumb D., Altieri B. et al. 2001, *A&A*, 365, L1
- Jiménez-Bailón E., et al., 2006, *AN*, 327, 1059
- Jiménez-Bailón E., Piconcelli E., Guainazzi M., Scharrel N., Rodríguez-Pascual P. M., Santos-Lleó M., 2005, *A&A*, 435, 449
- Kaspi S., et al., 2002, *ApJ*, 574, 643
- Kendall, M.G., & Stuart, A., *The advanced Theory of Statistics Vol. 2*, Hafner, New York, Section 19.26, page 97
- Kinkhabwala A., et al., 2002, *ApJ*, 575, 732
- Krongold Y., Jiménez-Bailón E., Santos-Lleó M., Nicastro F., Elvis M., Brickhouse N., Andrade-Velazquez M., Binette L., Mathur S., 2008, *ApJ* (submitted)
- Krongold Y., Nicastro F., Elvis M., Brickhouse N., Binette L., Mathur S., Jiménez-Bailón E., 2007, *ApJ*, 659, 1022
- Krongold Y., Nicastro F., Brickhouse N. S., Elvis M., Liedahl D. A., Mathur S., 2003, *ApJ*, 597, 832
- Longinotti A. L., de La Calle I., Bianchi S., Guainazzi M., Dovciak M., 2007, arXiv, 709, arXiv:0709.3268
- Magdziarz P., Zdziarski A. A., 1995, *MNRAS*, 273, 837
- Mathur S., 1994, *ApJ*, 431, L75
- McKernan B., Yaqoob T., Reynolds C. S., 2007, *MNRAS*, 379, 1359
- Miller, J. M. 2007, *ARAA*, 45, 441
- Miniutti G., et al., 2007, *PASJ*, 59, 315
- Mulchaey J. S., Wilson A. S., Tsvetanov Z., 1996, *ApJS*, 102, 309
- Nandra K., O'Neill P. M., George I. M., Reeves J. N., 2007, *MNRAS*, 382, 194
- Nandra, K. 2006, *MNRAS*, 368, L62
- Netzer H., et al., 2003, *ApJ*, 599, 933
- Perola G. C., Matt G., Cappi M., Fiore F., Guainazzi M., Maraschi L., Petrucci P. O., Piro L., 2002, *A&A*, 389, 802
- Piconcelli E., et al., 2006, *A&A*, 453, 839
- Piconcelli, E., Jimenez-Bailón, E., Guainazzi, M., Scharrel, N., Rodríguez-Pascual, P. M., & Santos-Lleó, M. 2005, *A&A*, 432, 15
- Piconcelli, E., Jimenez-Bailón, E., Guainazzi, M., Scharrel, N., Rodríguez-Pascual, P. M., & Santos-Lleó, M. 2004, *MNRAS*, 351, 161
- Pounds K. A., Reeves J. N., 2007, *MNRAS*, 374, 823
- Reeves J., Done C., Pounds K., Terashima Y., Hayashida K., Anabuki N., Uchino M., Turner M., 2008, *MNRAS*, 385, L108
- Reeves J. N., Porquet D., Turner T. J., 2004a, *ApJ*, 615, 150
- Reeves J. N., O'Brien P. T., Ward M. J., 2003, *ApJ*, 593, L65
- Revnivtsev M., Sazonov S., Jahoda K., Gilfanov M., 2004, *A&A*, 418, 927
- Reynolds, C. S., & Fabian, A. C. 1995, *MNRAS*, 273, 1167
- Risaliti G., Bianchi S., Matt G., Baldi A., Elvis M., Fabiano G., Zezas A., 2005, *ApJ*, 630, L129
- Sambruna R. M., Netzer H., Kaspi S., Brandt W. N., Chartas G., Garmire G. P., Nousek J. A., Weaver K. A., 2001, *ApJ*, 546, L13
- Sazonov S. Y., Revnivtsev M. G., 2004, *A&A*, 423, 469
- Scharrel, N., Rodríguez-Pascual, P. M., Santos-Lleó, M., Ballo, L., Clavel, J., Guainazzi, M., Jiménez-Bailón, E., & Piconcelli, E. 2007, *A&A*, 474, 431
- Scharrel, N., Rodríguez-Pascual, P. M., Santos-Lleó, M., Clavel, J., Guainazzi, M., Jiménez-Bailón, E., & Piconcelli, E. 2005, *A&A*, 433, 455
- Shemmer O., Netzer H., 2002, *ApJ*, 567, L19
- Schmid H. M., Appenzeller I., Burch U., 2003, *A&A*, 404, 505
- Schurch N. J., Done C., 2006, *MNRAS*, 371, 81
- Steenbrugge K. C., et al., 2005, *A&A*, 434, 569
- Tanaka Y., et al., 1995, *Natur*, 375, 659
- Veron-Cetty M.-P., Veron P., 2006, *yCat*, 7248, 0
- Williams R. J., et al., 2005, *ApJ*, 631, 856
- Wilms J., Pottschmidt K., Gleissner T., Nowak M. A., Heindl W. A., 2002, *AGAb*, 19, 33
- Winkler, H., Glass, I. S., van Wyk, F., Marang, F., Jones, J. H. S., Buckley, D. A. H., & Sekiguchi, K. 1992, *MNRAS*, 257, 659
- Young A. J., Lee J. C., Fabian A. C., Reynolds C. S., Gibson R. R., Canizares C. R., 2005, *ApJ*, 631, 733